Available online at www.sciencedirect.com

ScienceDirect

Mendeleev Commun., 2024, **34**, 342–344

Mendeleev Communications

Electroconductive expanded graphite–polyimide composite

Natalia S. Eroshenko, Veronica E. Andreeva,* Oleg A. Medennikov and Nina V. Smirnova

Platov South-Russian State Polytechnic University, 346428 Novocherkassk, Russian Federation.
E-mail: Veronica_a@mail.ru

DOI: 10.1016/j.mencom.2024.04.010

Expanded graphite–polyimide composites for fuel cells containing from 0 to 23 wt% expanded graphite were produced by direct compression molding after pre-mixing the binder and filler. The percolation threshold in this system was determined to be 2.5%, while the corrosion current was 3×10^{-2} μA cm^{-2}, and the composites were thermally stable up to 400 °C.

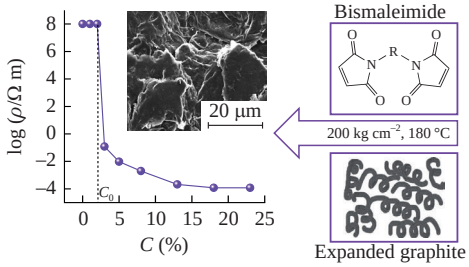

Keywords: bipolar plates, conductive polymer composites, expanded graphite, polyimide, fuel cell, percolation threshold.

Hydrogen power represents a modern approach to finding clean energy sources. Fuel cells are attractive for use in a variety of systems, including power supplies in the automotive and military applications, due to their high efficiency, significant power, low operating temperatures and fast start-up.[1]

An important element of fuel cell technology is bipolar plates. They are responsible for the quality of electrical contact between individual cells, uniform distribution of fuel and oxidizer, heat removal and mechanical strength of the fuel cell stack structure. To meet the functional requirements, ideal bipolar plates should have the characteristics of high thermal/electrical conductivity, corrosion resistance, low density, good mechanical properties, low cost and easy processing.[2] However, currently produced bipolar plates have drawbacks such as poor corrosion resistance and conductivity, high manufacturing cost and short service life.[3] It is well known that bipolar plates for low temperature proton exchange membrane fuel cells can be metal, graphite or composite. Each material finds its application depending on the task at hand. For example, metal bipolar plates have good electrical conductivity and bending strength but are prone to corrosion, while graphite bipolar plates have low density but are brittle.[4] Polymer–graphite composite bipolar plates have low cost and good corrosion resistance.[5] The electrical conductivity of a composite material is determined by the conductive filler, and the mechanical properties (bending strength, compression), chemical resistance in aggressive media and heat resistance are determined by the polymer binder (matrix).[1,6–8]

To produce polymer composite materials (PCMs), carbon-based fillers (*e.g.*, graphene, carbon nanotubes), which have excellent electrical and thermal properties, are usually added to the polymer matrix.[9,10] Thermally expanded graphite (EG) is a promising three-dimensional carbon filler with electrically conductive properties[11,12] and has a wide range of applications such as sensors, batteries,[13] supercapacitors[14] and additive manufacturing of functional materials.[15] EG particles consist of packs of graphene layers ranging in size from 10 to 200 nm; the length of the 'worms' can reach hundreds of micrometers. The degree of expansion determines the bulk density of EG, which can vary from 1 to 100 g dm^{-3}.

Both thermosetting and thermoplastic resins are used as polymer binders. Compared to thermoplastic binders, the use of thermosetting ones is due to the technological simplicity of obtaining an electrically conductive material. A peculiarity of thermosetting binders is a large number of functional groups capable of polycondensation and the formation of a rigid three-dimensional matrix, which determines high strength, thermal and chemical properties. The most common are hot-curing epoxy resins and phenol-formaldehyde resins. But their application is most often limited to operating temperatures, which do not exceed 120–160 °C. To eliminate this disadvantage and make it possible to operate electrically conductive materials at temperatures above 200 °C in aggressive environments, thermosetting polyimide binders are used.[16]

Bismaleimide monomers contain two reactive maleimide groups, which can undergo homopolymerization and copolymerization to form a densely cross-linked polymer network (glass transition temperature 250–300 °C), which determines their improved thermal and mechanical properties.[17] Thus, the goal of this work is to obtain composites based on EG and a high-temperature polyimide binder (PI), which would be characterized by a low content of filler and improved thermal and electrical properties. For this purpose, PCMs with different EG contents were prepared. The structure of the initial EG and the resulting EG–PI composites was studied by scanning electron microscopy (SEM).[†] The electrical resistance of the composites was determined and discussed in terms of the percolation theory. Their thermal properties and resistance to electrochemical corrosion were studied in detail.

To obtain PCM samples, thermosetting bismaleimide of the ITEKMA SB332 brand was used. Thermally expanded graphite produced by Silur LLC, grade EG-M, with a bulk density of 5 g dm^{-3} was used as an electrically conductive filler. The binder was mixed with the electrically conductive filler using the solution method.[‡] PCMs were prepared by direct compression molding

[†] SEM images of the materials under study were obtained using a Quanta 200 scanning electron microscope in the backscattered electron imaging mode.

[‡] For details, see Online Supplementary Materials.

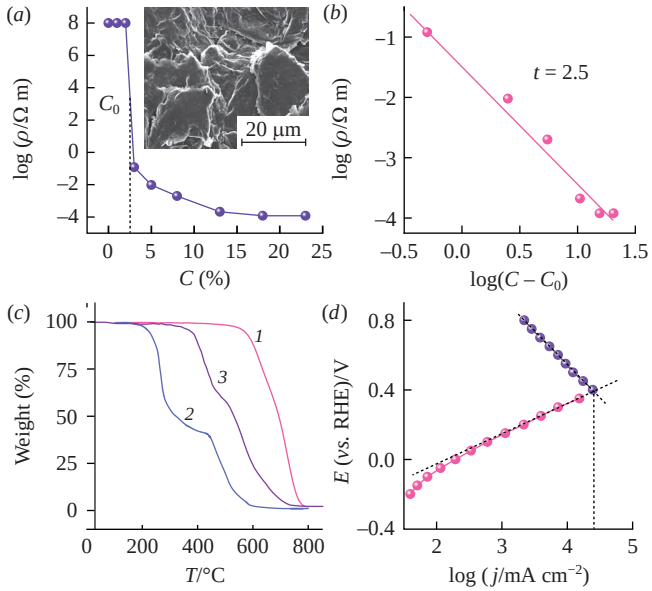

Figure 1 (*a*) Graph of volume resistance of the EG–PI composites *vs.* EG content. Inset: SEM image of the EG–PI composite. (*b*) Graph of the logarithm of the specific electric resistance of the EG–PI composites *vs.* the logarithm of the difference between the volume fraction of the conductive filler (*C*) and the percolation threshold (C_0). (*c*) TGA curves of (*1*) PI, (*2*) EG and (*3*) EG–PI. (*d*) Evans diagram of the EG–PI composite.

after pre-mixing of the binder and filler.[‡] In this work, the electrochemical characteristics of PCM were obtained[§] in an electrolyte solution of H_2SO_4 (pH 3) + 0.1 ppm HF.

The electrical resistivity ρ of the PCM, measured using a conventional four-point probe conductivity measurement device, is shown in Figure 1(*a*) as a function of the expected EG content in the EG–PI composites. The dependence of conductivity on the EG content is represented in Figure S1 (see Online Supplementary Materials). The morphology of the PCM was studied using SEM [Figure 1(*a*), inset]. The character of the curve allows us to distinguish three sections: a high-resistance section in which the resistivity of the system changes slightly, a section of maximum change $\rho(C)$ and an interval of minimum electrical resistance, which fully corresponds to the percolation theory and allows us to analyze the process of percolation cluster formation in the system under consideration.[18] The percolation transition concentration C_0 is defined as the point of intersection of the straight lines approximating the decreasing part of the $\rho(C)$ characteristics and the low-resistance branch of the experimental curve. For the EG–PI composite, the percolation transition occurs at a filler content of 2.5% [see Figure 1(*a*)]. A stable conductivity value of ~100 S cm^{-1} is observed at an EG content above 18 wt%.

Similar C_0 values were obtained for composites of EG with epoxy resin[19] and coal ash.[20] The percolation mechanism is described by a power law, which represents the dependence of the material resistance on the concentration of the conductive component. When the probability of filling the network elements is below the threshold at which a change in the state of the system occurs, network properties may be unconnected or isolated, and above the threshold, cohesive clusters appear, forming continuous regions. The dependencies are described by the following equation (1):

$$\rho(C) \sim \rho_0(C - C_0)^t, \quad (1)$$

where ρ_0 is the specific electrical resistance of the electrically conductive component, C and C_0 are the arbitrary and critical concentrations of the electrically conductive phase, respectively, t is the critical conductivity index, which is usually related to the dimensionality of the object.[21] The critical index t, determined by the tangent of the angle of slope of the straight line, is equal to 2.5 [Figure 1(*b*)]. The obtained value of t is typical for systems described by the percolation theory.[22]

In addition, the percolation threshold depends on the geometry of the conductive phase particles.[5] Worm-shaped particles of EG have pronounced geometric anisotropy. The length-to-diameter ratio for the EG particles in the composite is 100–300. This shape of particles allows the formation of a greater number of contacts between them and is a significant advantage compared to spherical or ellipsoidal particles.[5]

The thermal stability of EG–PI composites is critical when they are used at elevated temperatures. For example, for fuel cells it is extremely important to maintain the rigidity and accuracy of the geometry of the bipolar plates in the face of possible localized overheating during fuel cell operation. The thermal stability of the EG–PI composite was investigated. Figure 1(*c*) shows the TGA curves of EG, PI and EG–PI composite containing 5% filler. EG, obtained through intense chemical and thermal exposure, is characterized by a rather low oxidation onset temperature of 190 °C. The weight loss of EG at 190–430 °C is associated with the thermal decomposition of a large number of surface oxygen-containing functional groups, such as quinone, carboxyl, hydroxyl, *etc.*[18] Further weight loss at a temperature of 430–650 °C occurs due to the combustion of carbon. The thermal decomposition of PI and EG–PI composite begins at 425 °C. Such high thermal stability of the polymer composite may be due to the insulation of the EG surface by the polymer component and its low mass fraction in the composite. Thus, the resulting composites meet the requirements of increased thermal stability.

When using composites as bipolar plates of fuel cells, a necessary condition is their high corrosion resistance. To determine the corrosion current of composite materials, stationary potentiostatic polarization curves were obtained, plotted in semi-logarithmic coordinates (Evans diagram) [Figure 1(*d*)]. The calculated value of the corrosion resistance is 3×10^{-2} μA cm^{-2}, which is significantly lower than the U.S. Department of Energy (DOE) requirement of 0.1 μA cm^{-2} (Table 1).[23]

In conclusion, the EG–PI composites were prepared by direct compression molding after preliminary mixing of the PI binder and the EG filler using a solution method. The conductivity of the composite is determined by a conductive network of EG particles. The percolation threshold of the composites is 2.5 wt%. The structural feature, *i.e.*, the high aspect ratio of the EG particles, plays an important role in the formation of the conductive network within the PI matrix. High thermal stability up to 400 °C and extremely low corrosion current of 3×10^{-2} μA cm^{-2} allow us to consider this EG–PI composite containing 5 wt% EG as a promising material for the manufacture of bipolar plates of fuel cells.

The work was carried out within the framework of the strategic project ‘Hydrogen Energy Systems’ of the Development Program of SRSPU (NPI) as part of the implementation of the strategic academic leadership program ‘Priority-2030’.

Table 1 Technical parameters of bipolar plates.

Data source	Electrical conductivity/S cm^{-1}	Corrosion current/μA cm^{-2}		Flexural strength/MPa
		Anode	Cathode	
DOE[a]	> 100	–[b]	< 0.1	> 34
This work	260	–[b]	3×10^{-2}	390

[a] Reference 23. [b] No active peak.

[§] All tests were performed using an Electrochemical Instruments P20 CV potentiostat (see Online Supplementary Materials).

Online Supplementary Materials

Supplementary data associated with this article can be found in the online version at doi: 10.1016/j.mencom.2024.04.010.

References

1 *Handbook of Fuel Cells: Fundamentals, Technology and Applications*, eds. W. Vielstich, A. Lamm and H. A. Gasteiger, Wiley, New York, 2003, vol. 4.
2 Q.-L. Yan, M. Gozin, F.-Q. Zhao, A. Cohen and S.-P. Pang, *Nanoscale*, 2016, **8**, 4799.
3 P. Sharma and O. P. Pandey, in *PEM Fuel Cells: Fundamentals, Advanced Technologies, and Practical Application*, ed. G. Kaur, Elsevier, Amsterdam, 2021, pp. 1–24.
4 R. K. Gautam, S. Banerjee and K. K. Kar, *Recent Pat. Mater. Sci.*, 2015, **8**, 15.
5 F. Tarannum, S. Danayat, A. Nayal, R. Muthaiah, R. S. Annam and J. Garg, *Mater. Chem. Phys.*, 2023, **298**, 127404.
6 J. G. Clulow, F. E. Zappitelli, C. M. Carlstrom, J. I. L. Zemsky, D. N. Busick and M. S. Wilson, *AIChE Spring National Meeting 'Fuel Cell Technology: Opportunities and Challenges'*, New Orleans, LA, 2002, p. 417.
7 V. V. Aleshkevich, B. A. Bulgakov, Y. V. Lipatov, A. V. Babkin and A. V. Kepman, *Mendeleev Commun.*, 2022, **32**, 327.
8 R. B. Salikhov, R. A. Zilberg, I. N. Mullagaliev, T. R. Salikhov and Y. B. Teres, *Mendeleev Commun.*, 2022, **32**, 520.
9 M. Saeidijavash, J. Garg, B. Grady, B. Smith, Z. Li, R. J. Young, F. Tarannum and N. B. Bekri, *Nanoscale*, 2017, **9**, 12867.
10 F. Tarannum, S. S. Danayat, A. Nayal, R. Muthaiah, R. S. Annam and J. Garg, *Nanomaterials*, 2022, **12**, 1877.
11 A. M. Khanov, L. E. Makarova, A. I. Degtyarev, D. M. Karavaev, D. V. Smirnov and O. Yu. Isaev, *Izvestiya Samarskogo nauchnogo tsentra Rossiiskoi akademii nauk* (*Izvestia of Samara Scientific Center of the Russian Academy of Sciences*), 2011, **13**, no. 4–4, 1119 (in Russian).
12 V. K. Kochergin, R. A. Manzhos, I. I. Khodos and A. G. Krivenko, *Mendeleev Commun.*, 2022, **32**, 492.
13 E. M. Masoud, A.-A. El-Bellihi, W. A. Bayoumy and E. A. Mohamed, *J. Mol. Liq.*, 2018, **260**, 237.
14 M. F. El-Kady, V. Strong, S. Dubin and R. B. Kaner, *Science*, 2012, **335**, 1326.
15 X. Wang, M. Jiang, Z. Zhou, J. Gou and D. Hui, *Composites, Part B*, 2017, **110**, 442.
16 F. Badrul, K. A. Abdul Halim, M. A. A. Mohd Salleh, M. F. Omar, A. F. Osman and M. S. Zakaria, *AIP Conf. Proc.*, 2021, **2347**, 020240.
17 R. R. Mukhametov, E. V. Dolgova, Yu. I. Merkulova and M. I. Dushin, *Aviatsionnye materialy i tekhnologii (Aviation Materials and Technologies)*, 2014, no. 4, 53 (in Russian).
18 F. Farivar, P. L. Yap, K. Hassan, T. T. Tung, D. N. H. Tran, A. J. Pollard and D. Losic, *Carbon*, 2021, **179**, 505.
19 N. Radouane and A. Maaroufi, in *Epoxy-Based Composites*, eds. S. J. S. Chelladurai, R. Arthanari and M. R. Meera, IntechOpen, London, 2022, pp. 45–58.
20 F. A. M. M. Gonçalves, M. Santos, T. Cernadas, P. Alves and P. Ferreira, *J. Mater. Sci.*, 2022, **57**, 15183.
21 B. I. Shklovskii and A. L. Efros, *Elektronnye svoistva legirovannykh poluprovodnikov (Electronic Properties of Doped Semiconductors)*, Nauka, Moscow, 1979 (in Russian).
22 A. Celzard, E. McRae, J. F. Marêché, G. Furdin, M. Dufort and C. Deleuze, *J. Phys. Chem. Solids*, 1996, **57**, 715.
23 [dataset] T. Benjamin, R. Borup, N. Garland, C. Gittleman, B. Habibzadeh, S. Hirano, D. Ho, G. Kleen, J. Kopasz, B. Lakshmanan, D. Masten, M. Mehall, D. Myers, S. Onorato, D. Papageorgopoulos, D. Peterson, J. Spendelow, J. Waldecker, A. Wilson and M. Zou, *Fuel Cell Technical Team Roadmap*, version Nov 2017, https://www.energy.gov/sites/prod/files/2017/11/f46/FCTT_Roadmap_Nov_2017_FINAL.pdf.

Received: 11th December 2023; Com. 23/7340